

A Different Perspective on the Solid Lubrication Performance of Black Phosphorous: Friend or Foe?

Matteo Vezzelli,* Manel Rodríguez Ripoll, Sabine Schwarz, Ali Erdemir, Maria Clelia Righi,* and Carsten Gachot*

Black phosphorous (BP), a promising 2D material with exceptional electronic and optical properties, has shown remarkable potential in tribology as an additive in liquid lubrication and a composite in solid lubrication. However, its potential as the standalone solid lubricant is still at its early stage. This study evaluates BP's solid lubrication performance as deposited coating (by drop casting) on a variety of metallic substrates (polished AISI 52 100 steel, aluminum, copper, and iron) under different contact pressures using a ball-on-disc linear-reciprocating test machine in dry conditions. The results demonstrate that BP does not systematically reduce friction and wear. Depending on the contact pressure and the characteristic of the substrate material (particularly surface roughness), its friction and wear behavior vary a great deal. The best results observed are a 33% reduction in friction with increased surface roughness on iron and a 23% reduction in wear on aluminum. While no general trend is observed for contact pressure effects, increased substrate roughness proves beneficial, enhancing lubricant retention and exploiting BP's low interlayer shear mechanism. Therefore, this study demonstrates that while promising, BP's solid lubrication performance is not exceptional. It also highlights the importance of optimizing test conditions and materials for enhanced lubrication.

Among these, 2D layered materials have garnered substantial interest due to their exceptional friction and wear properties compared to their 3D counterparts. It has been shown that these 2D materials, with only one or a few atomic layers, can dramatically reduce friction, thanks to their interlayer shear properties.^[5] The most extensively studied 2D materials in this context include transition metal dichalcogenides (such as MoS₂ and WS₂), hexagonal boron nitride, MXenes, graphene, and black phosphorous (BP).^[6–8]

In recent years, the monolayer form of BP, also known as phosphorene, has emerged as one of the most promising 2D materials, renowned for its exceptional electronic properties, including a tunable bandgap and high charge carrier mobility.^[9–11] Since 2018, the tribological properties of BP have attracted significant attention, with both theoretical and experimental studies focusing on its layered structure to further optimize its friction and wear performance.^[12–14]

Theoretical calculations have demonstrated that phosphorene layers can easily share against each other, due to strong in-plane covalent bonds and weak interlayer van der Waals forces.^[15] However, computational studies have evidenced the propensity of BP for oxidation, which enhances its hydrophilicity.^[16] Under these conditions, atomic force microscopy experiments have confirmed a reduction in friction and wear.^[17] However, it is crucial to recognize that these tribological observations are conducted

1. Introduction

Friction and wear play a crucial role in the efficiency and reliability of mechanical systems involving the relative motion of solid surfaces.^[1] These phenomena significantly impact various industries, from automotive to aerospace, influencing energy efficiency and system performance.^[2,3] In recent decades, besides the move widely used liquid lubricants, solid lubricants have also emerged as novel solutions to mitigate friction and wear challenges.^[4]


M. Vezzelli, M. C. Righi
Department of Physics and Astronomy "Augusto Righi"
University of Bologna
40127 Bologna, Italy
E-mail: matteo.vezzelli3@unibo.it; clelia.righi@unibo.it

M. Rodríguez Ripoll
AC2T Research GmbH
Viktor-Kaplan-Straße 2/C, 2700 Wiener Neustadt, Austria

S. Schwarz
USTEM
TU Wien
Wiedner Hauptstraße 8-10, 1040 Vienna, Austria

A. Erdemir
J. Mike Walker'66 Department of Mechanical Engineering
Texas A&M University
College Station, TX 77843, USA

C. Gachot
Institute of Engineering Design and Product Development
TU Wien
1060 Wien, Austria
E-mail: carsten.gachot@tuwien.ac.at

 The ORCID identification number(s) for the author(s) of this article can be found under <https://doi.org/10.1002/adem.202401756>.

© 2024 The Author(s). Advanced Engineering Materials published by Wiley-VCH GmbH. This is an open access article under the terms of the Creative Commons Attribution-NonCommercial-NoDerivs License, which permits use and distribution in any medium, provided the original work is properly cited, the use is non-commercial and no modifications or adaptations are made.

DOI: 10.1002/adem.202401756

under idealized conditions at the nanoscale, potentially limiting their direct translation to macroscopic behavior or real-world applications.

At the macroscopic scale, BP has experimentally demonstrated versatility in different tribological applications. It has been used as an additive in both water- and oil-based liquid lubricants,^[18–21] as a solid filler in coatings,^[22,23] and composite materials.^[24,25] Despite variations of several orders of magnitude in tribological parameters such as applied load and sliding velocity across studies, BP consistently exhibited excellent friction and wear reduction properties.

Until now, only one recent study has investigated the tribological performance of BP as a standalone solid lubricant.^[26] In this work, BP coatings of two different thicknesses were tested in a ball-on-disc experiment under dry conditions. The results showed that BP coatings managed to reduce friction coefficient down to 0.2 level for the thicker coating and between 0.2 and 0.5 for the thinner coating compared to uncoated references, which exhibited friction coefficients from 0.2 to 0.8. While these results showed a promising performance for BP as a solid lubricant, they did not nevertheless examine the effects of substrate materials and the loading conditions (only applying a relatively low load of 50 mN, corresponding to about 250 MPa Hertzian contact pressure).

While previous research has represented a significant milestone, the potential of BP as a standalone solid lubricant remains largely unexplored, particularly under diverse tribological conditions including test materials, surface roughness, and higher contact pressures. Therefore, this work aims to expand the available data by subjecting BP to more demanding experimental conditions, enhancing its suitability for different applications. We systematically studied the tribological behavior of BP as a solid lubricant coating. The BP was deposited via drop casting and evaluated using a linear-reciprocating ball-on-disc setup. These tests were conducted on various metallic substrates (polished steel AISI 52 100, aluminum 99.5%, copper 99.95%, iron 99.85%) under two different load conditions (0.25 and 1 N) and chosen based on previous work,^[27] providing a more comprehensive understanding of BP's performance across a range of practical scenarios.

The results of this study further confirmed the effectiveness of BP in reducing friction and wear but not across all tribological conditions. Its performance is highly dependent on multiple factors, including the substrate material, applied normal load, surface roughness, coating deposition method, and other variables yet to be fully explored, such as ambient humidity and coating thickness. Our findings underscore the inherent complexity of 2D layered tribological systems and highlight the critical role of operating conditions in determining the lubricating effectiveness of BP coatings and solid lubricants in general. Finally, we emphasize the necessity of carefully considering these factors when investigating the feasibility of emerging solid lubricants.

2. Results and Discussion

2.1. Sample Characterization

To obtain the BP powder for characterization, 5 mL of the starting solution was centrifuged to remove most of the 2-propanol, and the remaining solution was evaporated under vacuum

through a Schlenk line to preserve sample flakes that might agglomerate during heating. Transmission electron microscopy (TEM) with energy-dispersive X-ray (EDS) analysis was then performed on several flakes. **Figure 1a** shows a representative BP flake. The two yellow arrows indicate the areas analyzed by selected-area electron diffraction (SAED), shown in panels (b) and (c), which confirm the presence of both crystalline (well-defined larger diffraction spots) and nanocrystalline phases (smaller spots), with measured orthorhombic planes of BP with zone axis in (b) [112] and (c) [231]. The TEM image in panel (d) is complemented by EDS chemical analysis in panels (e) and (f), revealing that the BP flake is mainly composed of phosphorous, with partial surface oxidation. Panel (g) presents a high-resolution TEM (HRTEM) image, clearly verifying the ordered layered structure of the pristine BP flake, with a measured inter-layer distance of 0.52 nm, close to the reported literature value of 0.53 nm.^[28–31]

To characterize the as-deposited BP coating on the steel substrate before tribological testing, X-ray photoelectron spectroscopy (XPS) measurements were performed. **Figure 2a** shows a broad P 2*p* peak at 134.6 eV, corresponding to various phosphorous oxide species like P=O and O–P=O,^[32–34] confirming the rapid oxidation of the surface under air exposure. Smaller peaks at 130.1 and 131.2 eV are attributed to the P 2*p*_{1/2} and P 2*p*_{3/2} doublet, respectively, arising from unoxidized P–P bonds found beneath the oxide coating.^[17,32] The oxygen O 1*s* spectrum in **Figure 2b** reveals the presence of two peaks at 532.0 and 533.6 eV, thus confirming the presence of oxide products. The peak at 532.0 eV corresponds to P=O dangling oxygen while the peak at 533.6 eV is attributed to bridging oxygen P–O–P.^[17,34] Several measurements found the ratio of total oxygen to phosphorous to be between 2.08 and 2.27. A stoichiometric oxygen:phosphorous ratio of 1.5 indicates the presence of P₂O₃, while a ratio of 2.5 corresponds to P₂O₅. Therefore, the phosphate oxides present on the surface are primarily a mixture of P₂O₃ and P₂O₅.^[17,34] **Figure 2c** shows weak iron oxide signals, indicating a minimal exposure of the substrate due to coverage by the BP coating.^[35–37] Moreover, **Figure 2d** reveals tin impurities, while weak fluorine signals were also detected. The tin and fluorine impurities likely originate from the BP synthesis processes.^[33,38–41] Other minor carbon impurities were also detected, which could arise from residual 2-propanol, atmospheric contamination, or the specimen holder used during characterization. Carbon and fluorine XPS images are available in **Figure S7**, Supporting Information.

The complementary XPS and TEM–EDS characterization results clearly confirm the presence of BP as the starting material and within the as-deposited coating on the steel substrate. Furthermore, it has been detected that significant surface oxidation occurs once the BP is exposed to air after removal from the protective solvent environment, mainly forming the oxide species P₂O₃ and P₂O₅.

2.2. Tribological Characterization

The first set of experiments was performed with the BP coating on a steel substrate (AISI 52 100). Friction coefficients (COF) were measured for both uncoated steel and BP-coated steel at two different applied loads, as shown in **Figure 3**.

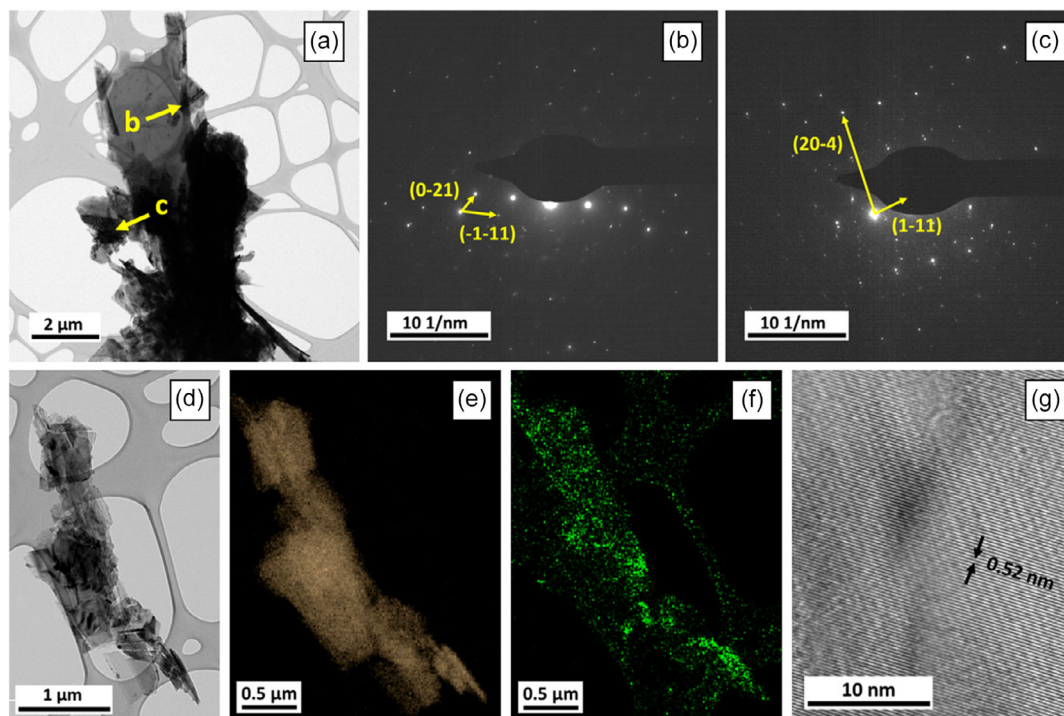


Figure 1. TEM and EDS analysis of BP powder. a) TEM images of a single BP flake, with yellow arrows corresponding to the b,c) SAED images. d) Additional TEM image of another flake and corresponding EDS mapping for e) phosphorous and f) oxygen. Panel g) provides a HRTEM image of the layered structure.

Comparing Figure 3a,b, the COF for the uncoated steel references is in the typical range of 0.6–0.8 for solid dry contacts and is slightly lower at higher loads, as reported by Bowden and Tabor.^[42] When BP is present, we observe a lower average COF value, more pronounced at 1 N. Looking in detail at the first few seconds of the experiment, the COF is a bit lower when applying 0.25 N. However, the high standard deviation of the measurements makes this reduction minimal; thus, we do not observe a significant reduction in friction when BP is present. A possible explanation could be that BP has poor adhesion to the polished steel surfaces and can be easily removed during sliding. In terms of wear, **Figure 4** shows the images of the substrates and the counterbodies for the corresponding steel and BP-coated steel tests.

The wear volume is higher in the case of the BP coating compared to the references for both loads (0.04 and 0.24 mm³ for 0.25 N, 0.09 and 0.47 mm³ for 1 N). In the uncoated steel substrate references (b) and (f), one can clearly identify wear debris distributed around the wear tracks (more significant at 1 N) due to the linear reciprocating motion. Regarding the BP coating counterbodies, they show less wear, especially at 1 N. Therefore, from this first experiment, we can deduce that the BP coating does not work effectively in terms of COF and wear reduction.

To further investigate the findings, Raman spectroscopy was performed on the sample tested at 0.25 N load, stopping the experiment after 1 min to avoid removing any potential tribofilm that may have formed (**Figure 5**).

Both Raman spectra in **Figure 5c,d** show the characteristic peaks located at 361.3, 439.4, and 465.9 cm⁻¹ corresponding to

the P atomic vibration modes.^[17,22,34] The intensity ratio between the A_g¹ and A_g² peaks is around 0.6 for both spectra, indicating a low degree of BP oxidation.^[43] The Raman spectrum of the unworn BP coating (**Figure 5c**) reveals a broad, low-intensity signal in the range of 800–1100 cm⁻¹, which can be attributed to oxidized BP species. After the tribological experiment, the Raman spectrum from within the wear track (**Figure 5d**) shows slightly more well-defined signals emerging in the same region, suggesting the presence of different types of oxide compounds that may have formed during the wear process. However, these signals are difficult to discern due to the higher baseline caused by the increased reflection from the exposed steel substrate without the coating. The optical Raman image of the wear track in **Figure 5b** reveals a yellow–blue–green colored region, which could arise from various phosphorous and iron compounds formed on the surface during sliding. To further investigate the nature of these species, complementary XPS measurements were performed (**Figure 6**), with the addition of depth analysis (**Figure S8**, Supporting Information).

After the sliding experiment, the peak at 134.6 eV (attributed to oxidized P) decreases significantly, while those at 129.9 and 130.8 eV (attributed to P–P bonding) increase (**Figure 6a**), suggesting the removal of the outermost phosphorous oxide layer. However, this seems inconsistent with the increased intensity of the peaks at 532.0 and 533.6 eV corresponding to oxygen species (**Figure 6b**). The increase in the oxygen signal could potentially be due to the appearance of iron oxide from the underlying steel substrate as the coating is worn away. Indeed, **Figure 6c** shows the characteristic doublet of Fe 2p_{1/2} and Fe 2p_{3/2} at around 724.3 and 710.5 eV, respectively, from Fe₂O₃. Further-

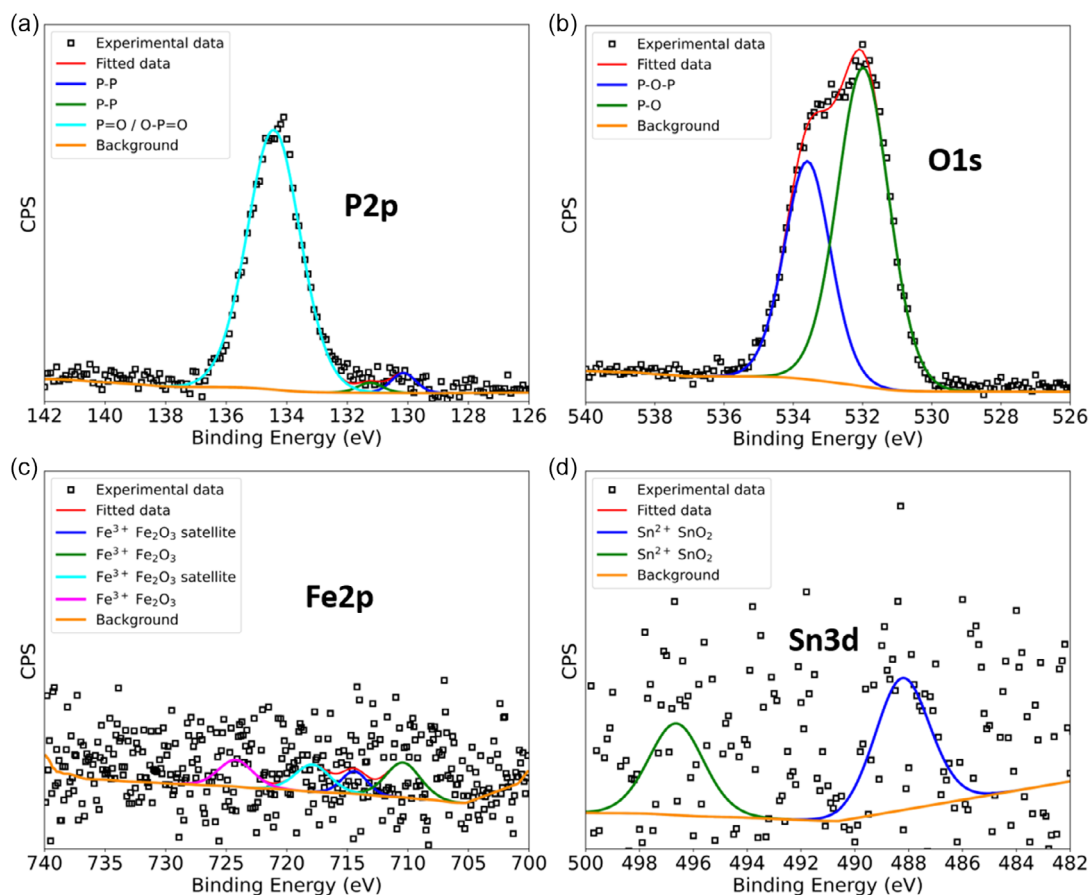


Figure 2. High-resolution XPS spectra of the BP coating over the steel substrate before the tribological experiment for a) phosphorous, b) oxygen, c) iron, d) tin.

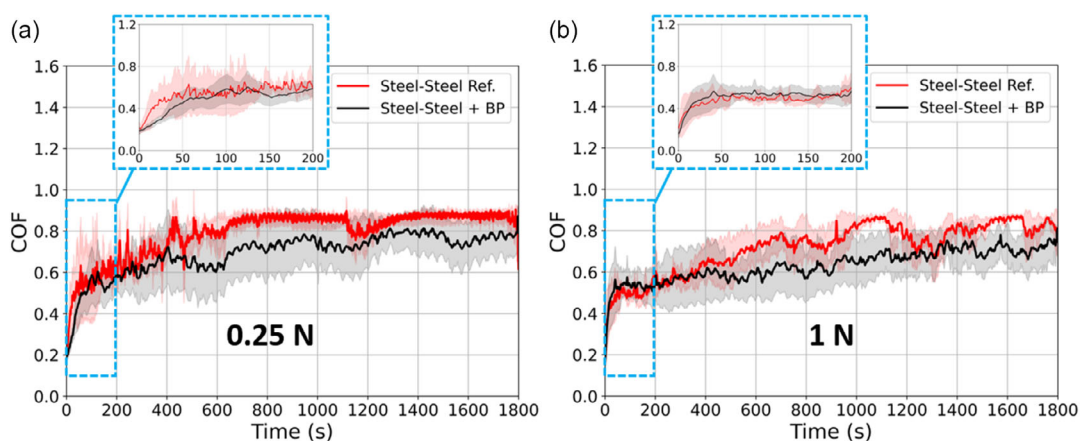


Figure 3. Evolution of the averaged COF (three single measurements) over time for the uncoated (reference) and BP-coated steel–steel tribopair at 0.25 N in panel a) and 1 N in panel b). The blue insets show the first 200 s of the test. The shaded areas around the curve represent the standard deviation.

more, a notable increase in both tin and fluorine signals was observed in the wear track following the sliding process. Figure 6d reveals strong tin signals, with Sn 3d peaks at 488.2 and 496.6 eV, corresponding to SnO₂.^[44] The presence of tin oxide could also account for the increased oxygen signal. The formation of SnO₂ observed in the XPS spectra after sliding

could be attributed to the energy input from the applied load and the heat generated during the sliding action, which may have overcome the activation barrier for its formation. Indeed, SnO₂ forms when tin is heated in the presence of air.^[45] However, in the Raman analyses, clear SnO₂ signals^[46] were not detected, probably because Raman spectroscopy has a lower depth resolution

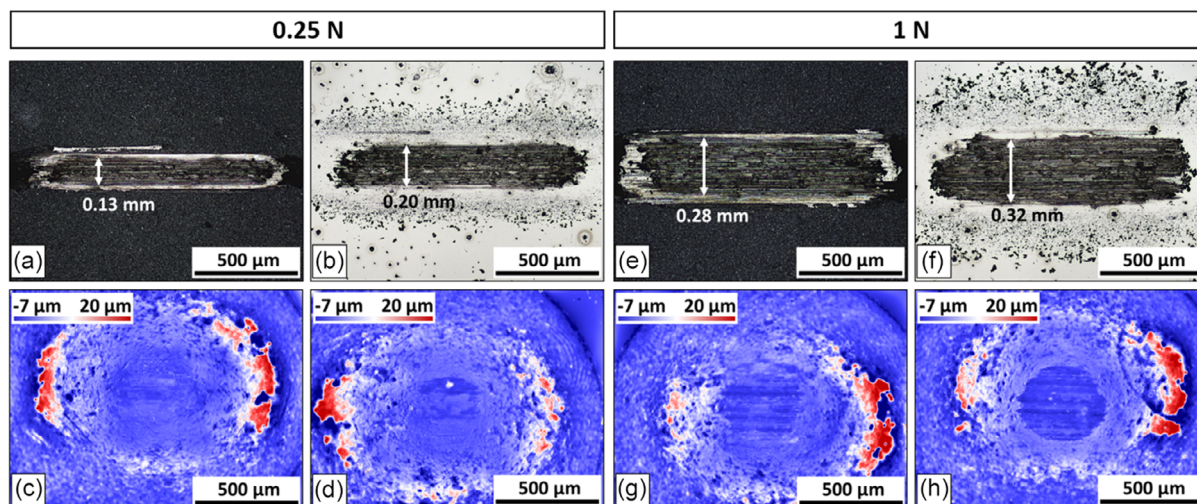


Figure 4. Wear measurements showing: a,e) the BP-coated steel substrate, b,f) the uncoated steel substrate references, c,g) the steel counterbodies used against the BP-coated samples, d,h) the steel counterbodies used against the uncoated reference samples.

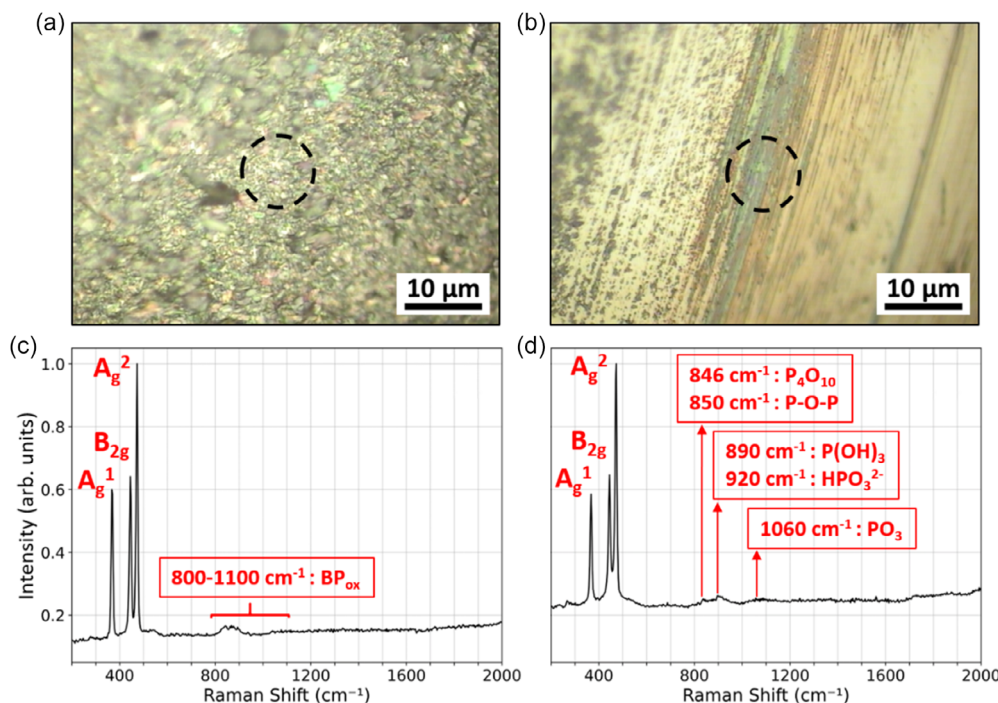


Figure 5. Raman images and spectra of the unworn BP-coated steel in panels a,c) and of the wear track in panels b,d), respectively. The black circles in images (a) and (b) indicate the measured spots. The red insets in spectra (c) and (d) show the potential candidate chemical species, according to reference data from the literature.^[17,34]

compared to XPS. The formation of tin oxide may have contributed to the slight COF reduction observed, and these effects could potentially be enhanced by different tribological conditions. Previous reports indicate that the presence of SnO₂ can reduce the COF and wear during tribological experiments when used as an oil additive.^[47] To the best of our knowledge, there are no prior studies on the use of SnO₂ as a solid lubricant. Therefore, further investigation may be useful to clarify whether SnO₂ can act as an effective solid lubricant under certain conditions.

We also evaluated the possible presence of FePO₄, since the study mentioned in Section 1^[26] demonstrated its tribochemical formation. Their XPS results showed Fe 2*p* signals at 714.7 and 728.8 eV, consistent with other XPS data for FePO₄.^[48] However, in our measurements (Figure 6c), we do not detect the signal at 728.8 eV. The differing tribological conditions in our experiment may have inhibited the formation of a FePO₄ tribofilm. These differences include five and twenty-fold increase in applied load (250 mN and 1 N vs. 50 mN, corresponding to Hertzian contact

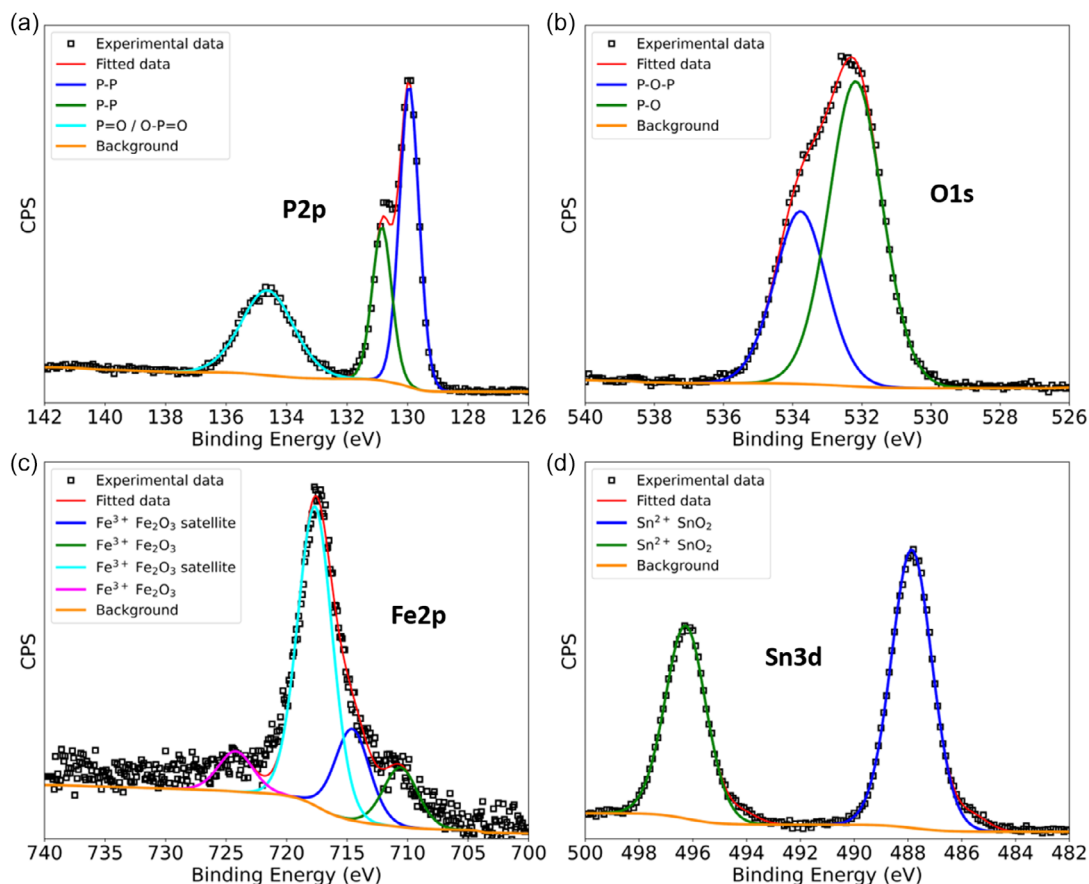


Figure 6. High-resolution XPS spectra of the BP-coated steel after the tribological experiment for a) phosphorous, b) oxygen, c) iron, d) tin.

pressures of 389.2 and 617.7 vs. 250 MPa, respectively), a 2.5 times reduction in sliding velocity (1 vs. 2.5 mm s⁻¹), and a different sample preparation and deposition method (drop casting instead of spray coating). Such significant differences in experimental parameters could account for the absence of the protective tribofilm observed in our study.

In addition to the previous analyses, infrared (IR) spectroscopy was performed on the samples tested at 0.25 and 1 N, stopping the experiment after 1 min. The resulting spectra (Figure S9, Supporting Information) exhibit similar profiles with two significant differences: a reduction in the signal at 3600 cm⁻¹, attributed to the removal of environmental moisture during sliding, and a decrease in the intensity of the signal at 1630 cm⁻¹, corresponding to the P=O bond, indicating the removal of the outermost phosphorus oxide layer. This latter observation aligns with the XPS findings.

Therefore, from this initial experiment, we believe that the minimal benefit in reducing friction and wear (only for the counterbodies) observed with BP is mainly due to the removal of the surface oxide layer by sliding and exposing more BP (increasing of the P-P contribution), potentially supported by other mechanochemical reactions such as SnO₂ formation. The durability of this lubricating effect is highly dependent on operating conditions like the applied load.

To further investigate the influence of the substrate material, another experiment was conducted with the BP coating deposited onto an aluminum substrate. Pure aluminum is known to be a less dense and more ductile metal than the used steel in our study. Consequently, the Hertzian contact pressure calculated in our steel-aluminum experiment is about 66% of that for steel-steel. **Figure 7** shows the evolution of the COF for the steel-aluminum tribopair. As observed, for both loads, the COF at the beginning is lower than the reference, increasing to about 0.7 after 125 and 75 s for 0.25 and 1 N, respectively. Compared to the experiment with the steel-steel tribopair, the COF is lower for a longer time. This may be due to the lower Hertzian pressure, which prolongs the adhesion of BP on the aluminum substrate. Additionally, the aluminum substrate has a root mean square height roughness (*S_q*) value 7.9 times larger than that of the polished steel, which could enhance the reservoir effect for the BP. This allows for a more gradual removal of BP during sliding, enabling phosphorene layers to slide against each other, thereby reducing friction.

Examining the wear shown in **Figure 8**, the wear volume is higher in the case of the BP coating compared to the references for 0.25 N (2.77 and 3.17 mm³), while for 1 N the BP coating shows less wear volume compares to the reference (8.71 and 6.69 mm³), with a reduction of 23%. As for the counterbodies, they seem to exhibit a lower wear, particularly at 0.25 N. Therefore, the

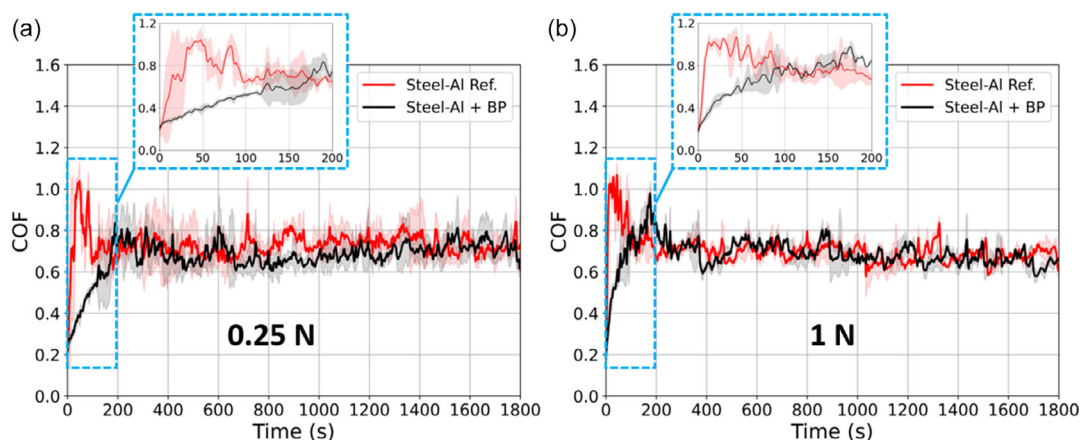


Figure 7. Evolution of the COF over time for the uncoated (reference) and BP-coated steel–aluminum tribopair at 0.25 N in panel a) and 1 N in panel b). The blue insets show the first 200 s of the test.

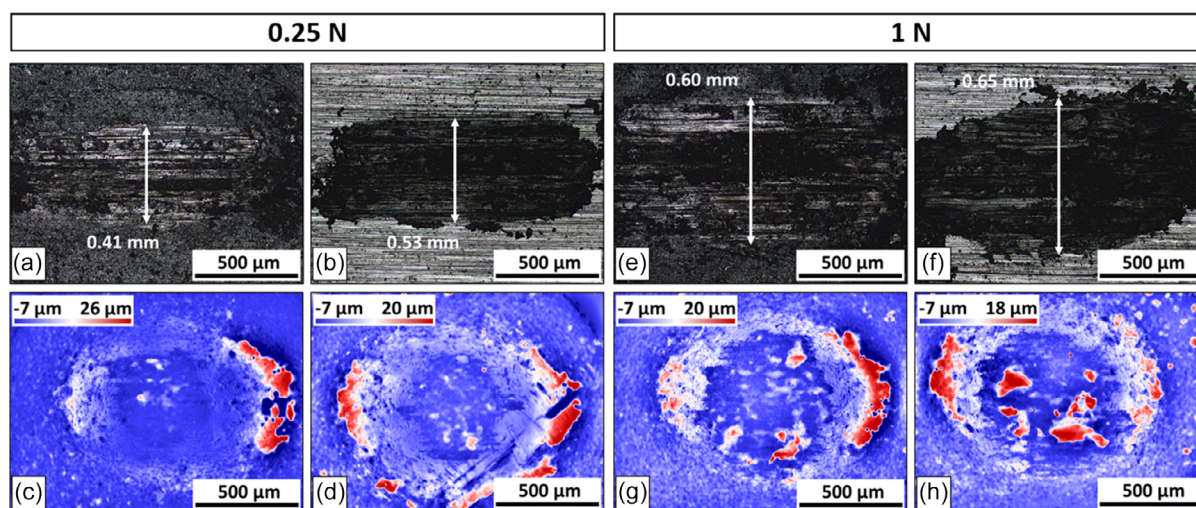


Figure 8. Wear measurements showing: a,e) the BP-coated aluminum substrate, b,f) the uncoated aluminum substrate references, c,g) the steel counterbodies used against the BP-coated samples, and d,h) the steel counterbodies used against the uncoated reference samples.

tribological performance of BP is better in this configuration, improved at lower load for COF and higher load for wear, compared to the previous steel-to-steel contact configuration.

Further analyses were carried out using TEM–EDS on the sample at 0.25 N, stopping the experiment after 1 min to avoid removing any tribofilm that may have formed. The focused ion beam (FIB) cut (Figure 9a) was performed in the middle of the wear track, and the cross-sectional morphology (Figure 9b) revealed well-defined crystalline domains with a measured orthorhombic plane of BP with the zone axis [001], as suggested by SAED (Figure 9c). The corresponding EDS line scan (Figure 9d) and elemental mappings (Figure 9e) confirm the presence of phosphorous, which is still partially oxidized. It can also be observed that where phosphorous is most abundant, there is less oxygen and vice versa. This may indicate that the lubricating effect of BP was primarily due to the removal of oxides, and the ductility of the aluminum substrate did not allow uniform removal, at least in the measured area. In addition, we could not see the presence of a tribofilm.

We also extended the tribological experiments by changing the metal substrate, focusing on copper and iron, to investigate the performance of BP over different metal substrates. The experiments on iron were conducted in polished and in scratched conditions to additionally evaluate the role of roughness as reservoir for solid lubricant, which also leads to a smaller local contact area.^[49] The results of these experiments are briefly discussed below and in more detail in the Section 1 and 2, Supporting Information.

Tribological experiments on copper substrate revealed a load-dependent correlation of the BP coating. At 0.25 N, the BP-coated sample exhibited a higher COF than the uncoated reference for the initial 1100 s (Figure S1, Supporting Information). Conversely, the 1 N test demonstrated a lower average COF compared to both the reference and the 0.25 N experiment.

Wear analysis (Figure S2, Supporting Information) revealed higher wear volume with the BP coating with respect to the references for 0.25 N (0.01 and 0.75 mm³) and 1 N (0.03 and

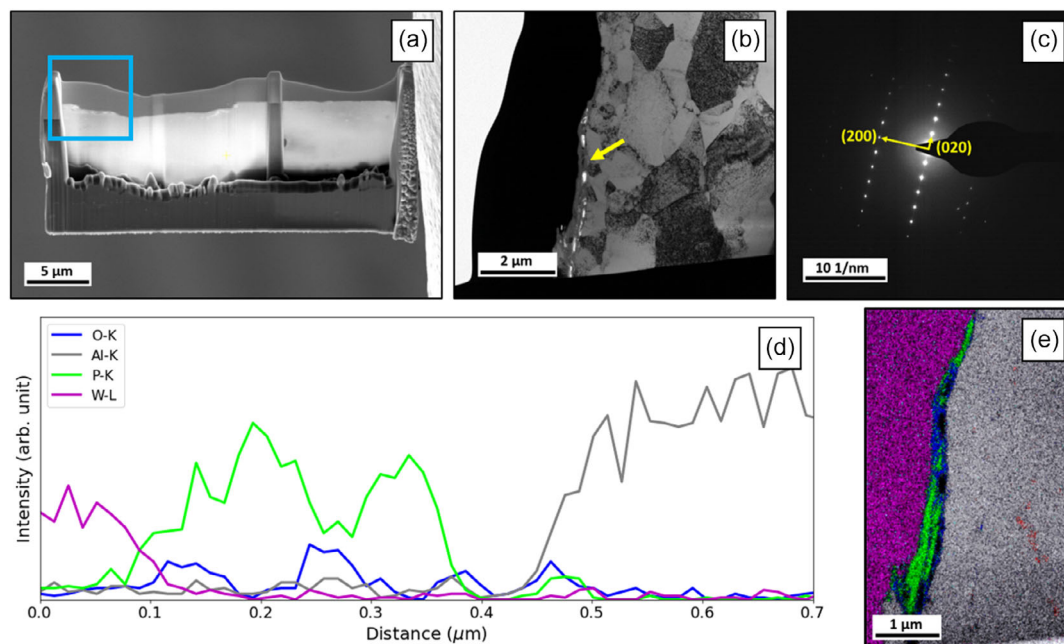


Figure 9. TEM and EDS analysis of the wear track after the steel–aluminum BP-coated experiment at 0.25 N and stopped after 1 min. a) FIB cross section of the wear track, with the blue square corresponding to the b) TEM image. The yellow arrow in panel (b) corresponds to the area of the c) SAED image. d) EDS line scan and e) elemental mapping of the section from panel (b) are also shown.

0.82 mm³), although this effect was less pronounced on the counterbodies.

These observations suggest two potential explanations. The increased COF at 0.25 N could be attributed to poor BP adhesion. In contrast, the reduced COF at 1 N might result from the higher mechanical energy input, potentially promoting interlayer sliding.

In conclusion, under the tested conditions, BP as a solid lubricant for the steel–copper tribopair did not significantly reduce friction and wear.

Tribological experiments on iron substrate revealed a load-dependent correlation of the BP coating. The reference samples showed typical running-in behavior, with COF stabilizing around 0.6 after initial oxide layer removal (Figure S3, Supporting Information). At 0.25 N, the BP-coated sample exhibited higher COF (0.8–1.0, peaking at 1.5) compared to the reference, eventually decreasing to 0.6–0.8 after 1400 s. The 1 N test showed lower COF values, peaking at 0.9 and reaching the reference level after 900 s.

Wear analysis (Figure S4, Supporting Information) demonstrated increased wear volume on BP-coated substrates and counterbodies for both loads compared to uncoated references. The wear was more pronounced at 0.25 N relative to its reference (0.01 and 0.95 mm³) than at 1 N (0.08 and 0.98 mm³), correlating with the higher COF observed at a lower load.

These results suggest that BP coating on polished iron substrate does not effectively reduce friction and wear, particularly at lower loads. We think that this behavior implies poor adhesion of BP to the iron surface. While higher loads may partially mitigate this effect through increased interlayer sliding of BP, the improvement is insufficient to outperform the uncoated reference.

Consequently, for the steel–iron tribopair as well, the use of BP as a solid lubricant under the tested conditions did not reduce friction and wear.

The effect of surface roughness on BP coating performance was investigated using manually ground iron samples with ≈ 12.7 times higher roughness than polished steel. Tribological tests revealed that BP-coated rough surfaces exhibited improved friction reduction compared to polished samples (Figure S5, Supporting Information). At 0.25 N, the COF was lower than the reference for the first 900 s, while at 1 N, a persistent 33% COF reduction was observed for the first 1400 s.

Wear analysis (Figure S6, Supporting Information) showed an increase in wear volume for BP-coated samples compared to uncoated references (0.12 and 0.36 mm³ for 0.25 N, 0.21 and 0.63 mm³ for 1 N), with similar wear on counterbodies. Notably, the wear volume increase did not correlate with the observed lower COF values.

We propose that increased surface roughness provides cavities for BP, acting as a reservoir and improving BP's durability and adhesion. This configuration enhances BP's friction reduction performance, particularly at higher loads where increased mechanical energy may promote interlayer sliding. In addition, the increased roughness results in a smaller local contact area with the underlying substrate, increasing the effective contact pressure and potentially promoting some tribochemical reactions.

Conclusively, under these experimental conditions, the increase in surface roughness of the substrate significantly enhanced the performance of BP as a solid lubricant in reducing friction, although no evident benefit in wear reduction was measured. These findings highlight the importance of surface topography in optimizing BP coating performance.

3. Conclusion

This study investigated the tribological behavior of BP as a stand-alone solid lubricant coating using linear-reciprocating ball-on-disc experiments. The tests were conducted on various metallic substrates (steel, aluminum, copper, iron) under different load conditions (0.25 and 1 N).

The results show that BP does not systematically reduce friction and wear. Its effectiveness is highly dependent on the metallic substrate and applied load. The benefits in friction reduction were attributed to the removal of the BP oxide layer, which exposed more BP for sliding, and the increased roughness of the substrate, which significantly enhanced BP adhesion by creating cavities that retained the lubricant, promoting more effective sliding between BP layers. However, no general trend was found for wear on either substrate or counterbodies. XPS, Raman, and TEM-EDS analyses did not reveal tribofilm formation. Additionally, no general correlation between performance and applied load was observed. Surprisingly, the formation of SnO₂ and enrichment in the wear scar was measured postsliding, originating from tin impurities in BP synthesis, potentially affecting its performance.

Overall, these results suggest that BP may perform better on surfaces with increased roughness, as its durability and adhesion may be more beneficial.

In conclusion, further research is needed to elucidate the fundamental mechanisms governing BP's tribological performance under different experimental conditions, such as different environmental conditions (e.g., under nitrogen/vacuum atmosphere, higher temperatures), different coating depositions (e.g., electro-spraying, electrophoretic deposition), and higher applied loads. This work contributes to the understanding of BP as a potential standalone solid lubricant and offers directions for future studies in this field.

4. Experimental Section

Sample and Substrates: The BP sample was purchased from Smart-Elements GmbH in the form of single- and multi-layered crystals dispersed in 2-propanol. The BP solution was prepared by sonication of high-quality BP crystals synthesized by chemical vapor transport method.^[38] The resulting concentration was 200 mg L⁻¹, with a lateral size ranging from 5 to 100 nm and a thickness of 1–10 layers. Since it is well known that it readily oxidizes on the surface under environmental conditions,^[17,50,51] few-layer BP is usually stored in organic solvents for protection.^[52] The used metallic substrates in this work are summarized in **Table 1**. The S_q values were measured with a 3D laser scanning microscope at the same magnification

level, and the polished steel was taken as a reference since it has the lowest absolute value. This ensured the calculation of a relative ΔS_q value for the roughness to compare the different substrates.

Deposition Method: Prior to the deposition of BP onto test samples, the sample solution was concentrated five times to 1000 mg L⁻¹ and sonicated in a water bath for at least 15 min to improve the stability of colloidal dispersion. It was found that longer sonication times did not improve dispersion stability. Drop casting using a micropipette was performed as a simple alternative to spray coating, as it was found to be easier for the deposition of BP on the metallic substrates. The resulting coating was homogeneous, with a measured thickness of ≈1.85 ± 0.93 μm. Before each new tribological test, the substrate with the coating was heated to 250 °C on a hot plate for 2 min to ensure that most of the products of 2-propanol were removed and then cooled down to room temperature. This temperature was chosen based on the data reported by Benziger and Madix^[53] and on the decomposition temperature of BP.^[54,55]

Tribological Experiments: The tribological experiments were performed on an MFT-2000 Tribometer (*Rtec Instruments*) in linear-reciprocating mode under ambient conditions at a temperature of 23 ± 5 °C and a relative humidity of 25% ± 7% for 30 min (900 cycles). 100Cr6 steel balls (AISI 52 100) with a diameter of 6 mm were used as a counterbody. The stroke length was 1.0 mm with a frequency of 0.5 Hz, resulting in a sliding speed of 1 mm s⁻¹. The load was kept constant for all tests at 0.25 and 1 N, giving a different Hertzian contact pressure based on the tribopair, as shown in **Table 2**. Each experiment was repeated at least three times to ensure statistical reproducibility.

Instrumental Analyses: The powder extracted from the BP solution (for the initial characterization) and the surface layers of the wear track were analyzed by TEM. To precisely examine a defined area of the wear track, careful target preparation was essential. For this purpose, the TEM lamellae were prepared using a *ThermoFisher Scios II FIB*. The TEM investigations were conducted with a *TECNAI F20* operated at 200 kV with an X-FEG. TEM images were acquired with a *Gatan Rio16*, 30 fps full-HD camera, and high-angle-annular dark-field scanning transmission electron microscope images were obtained using a *Gatan DigiSTEM II*. EDS analysis was performed with an *EDAX-AMETEK Apollo XLTW SDD system*. Additionally, SAED patterns were performed for phase analysis. Further HRTEM imaging was carried out for phase analysis using Fourier transformation (FT) and measuring lattice spacings directly from the HRTEM images.

Table 2. Mean Hertzian contact pressure in MPa for each different tribopair.

Tribopair	0.25 N	1 N
Steel-Steel	389.2	617.7
Steel-Fe	394.6	626.3
Steel-Al	258.0	409.6
Steel-Cu	319.9	507.8

Table 1. Materials used in this work. The technical purity of steel is not reported since it has a standard composition. The roughness value is expressed as S_q. The difference between S_q for each material and the selected reference (polished steel AISI 52 100) is also calculated as ΔS_q.

Used material	Dimensions [mm]	Technical purity [%]	Hardness [HV]	S _q [μm]	ΔS _q
Polished steel AISI 52 100	15.30 × 15.30 × 0.77	–	690	0.18	–
Aluminum	15.50 × 15.50 × 1.96	99.50	15	1.45	7.9
Copper	25.22 × 10.15 × 1.00	99.95	50	0.94	5.2
Fe polished (Armco)	20.30 × 20.30 × 2.74	99.85	150	0.22	1.2
Fe scratched (Armco)	20.30 × 20.30 × 2.74	99.85	150	2.33	12.7

XPS analysis was conducted using a *Thermo Fisher Scientific Thetaprobe* equipped with a monochromatic Al K α X-ray source (1486.6 eV). A pass energy of 200 eV and a spectrum energy step size of ≈ 0.7 eV were applied. The X-ray spot on the sample surface had a diameter of 50 μm , and the map grid step size was likewise set to 50 μm . Prior to analysis, the entire map area was briefly sputter cleaned with 3 keV Ar ions. Peak fitting was performed with the Thermo Fisher Scientific Avantage Data System software using Gaussian/Lorentzian functions. The C 1s peak of adventitious carbon located at 284.8 eV was utilized as a binding energy reference.

For Raman analysis, a LabRam Aramis spectrometer from Horiba Jovin Yvon (Germany) with a wavelength of 532 nm and a laser power output of 13.5 mW was used. The spot size was 20 μm , and the measuring time 3 s.

For IR analysis, attenuated-total reflection FT infrared spectroscopy was performed on a Bruker Tensor 27 spectrometer (Ettlingen, Germany) with a diamond crystal accessory in the solid state.

Wear images of the substrate counterbody, surface roughness, wear volume, and coating thickness were acquired using a 3D laser scanning microscope (VK-X1100 from Keyence) at a magnification level of 10x.

Supporting Information

Supporting Information is available from the Wiley Online Library or from the author.

Acknowledgements

These results are part of the “Advancing Solid Interface and Lubricants by First Principles Material Design (SLIDE)” project that received funding from the European Research Council (ERC) under the European Union’s Horizon 2020 research and innovation program (grant agreement no. 865633). Part of this work was funded by the “Austrian COMET-Programme” (Project K2 InTribology2, no. 906860) and carried out at the “Excellence Centre of Tribology” (AC2T research GmbH).

Conflict of Interest

The authors declare no conflict of interest.

Author Contributions

Matteo Vezzelli: Conceptualization (lead); Data curation (lead); Formal analysis (lead); Investigation (lead); Methodology (lead); Visualization (lead); Writing—original draft (lead); Writing—review & editing (lead). **Manel Rodríguez Ripoll:** Investigation (equal); Writing—review & editing (equal). **Sabine Schwarz:** Investigation (equal). **Ali Erdemir:** Writing—review & editing (equal). **Maria Clelia Righi:** Resources (equal); Supervision (equal). **Carsten Gachot:** Conceptualization (lead); Project administration (lead); Resources (lead); Supervision (lead); Writing—review & editing (lead).

Data Availability Statement

The data that support the findings of this study are available from the corresponding author upon reasonable request.

Keywords

2D materials, black phosphorous, frictions, metals, solid lubricants, tribologies, wears

Received: July 24, 2024

Revised: September 2, 2024

Published online:

- [1] I. Hutchings, P. Shipway, in *Tribology: Friction and Wear of Engineering Materials*, Butterworth-Heinemann **2017**, ISBN: 978-0-08-100910-9.
- [2] A. A. Voevodin, J. P. O’Neill, J. S. Zabinski, *Surf. Coat. Technol.* **1999**, 116–119, 36.
- [3] K. Holmberg, A. Erdemir, *Tribol. Int.* **2019**, 135, 389.
- [4] C. Donnet, A. Erdemir, *Surf. Coat. Technol.* **2004**, 180–181, 76.
- [5] S. Zhang, T. Ma, A. Erdemir, Q. Li, *Mater. Today* **2019**, 26, 67.
- [6] P. C. Uzoma, H. Hu, M. Khadem, O. V. Penkov, *Coatings* **2020**, 10, 897.
- [7] B. R. Manu, A. Gupta, A. H. Jayatissa, *Materials* **2021**, 14, 1630.
- [8] R. Wang, F. Zhang, K. Yang, Y. Xiong, J. Tang, H. Chen, M. Duan, Z. Li, H. Zhang, B. Xiong, *Adv. Colloid Interface Sci.* **2023**, 321, 103004.
- [9] S. Fan, J. Li, H.-Q. Cao, X. Liu, M. Cao, T. Liu, T. Xu, J. Su, *J. Mater. Chem. C* **2022**, 10, 14053.
- [10] H. Kim, S. Z. Uddin, D.-H. Lien, M. Yeh, N. S. Azar, S. Balendhran, T. Kim, N. Gupta, Y. Rho, C. P. Grigoropoulos, K. B. Crozier, A. Javey, *Nature* **2021**, 596, 232.
- [11] X. Ling, H. Wang, S. Huang, F. Xia, M. S. Dresselhaus, *Proc. Natl. Acad. Sci.* **2015**, 112, 4523.
- [12] G. Boidi, B. Ronai, D. Heift, F. Benini, M. Varga, M. C. Righi, A. Rosenkranz, *Adv. Colloid Interface Sci.* **2024**, 328, 103180.
- [13] F. Lv, W. Wang, J. Li, Y. Gao, K. Wang, *Friction* **2024**, 12, 823.
- [14] W. Wang, G. Xie, J. Luo, *Friction* **2018**, 6, 116.
- [15] G. Losi, P. Restuccia, M. C. Righi, *2D Mater.* **2020**, 7, 025033.
- [16] F. Benini, N. Bassoli, P. Restuccia, M. Ferrario, M. C. Righi, *Molecules* **2023**, 28, 3570.
- [17] S. Wu, F. He, G. Xie, Z. Bian, J. Luo, S. Wen, *Nano Lett.* **2018**, 18, 5618.
- [18] Q. Wang, T. Hou, W. Wang, G. Zhang, Y. Gao, K. Wang, *Friction* **2022**, 10, 374.
- [19] W. Tang, Z. Jiang, B. Wang, Y. Li, *Friction* **2021**, 9, 1528.
- [20] Z. Luo, J. Yu, Y. Xu, H. Xi, G. Cheng, L. Yao, R. Song, K. D. Dearn, *Friction* **2021**, 9, 723.
- [21] G. Tang, F. Su, X. Xu, P. K. Chu, *Chem. Eng. J.* **2020**, 392, 123631.
- [22] Y. Liu, J. Li, J. Li, S. Yi, X. Ge, X. Zhang, J. Luo, *ACS Appl. Mater. Interfaces* **2021**, 13, 31947.
- [23] S. Peng, Y. Guo, G. Xie, J. Luo, *Appl. Surf. Sci.* **2018**, 441, 670.
- [24] Z. Wang, L. Zhu, G. Xie, X. Ren, *J. Mater. Eng. Perform.* **2022**, 31, 9972.
- [25] Y. Lv, W. Wang, G. Xie, J. Luo, *Tribol. Lett.* **2018**, 66, 61.
- [26] G. Boidi, D. F. Zambrano, M. Varga, D. Heift, A. Rosenkranz, *Appl. Surf. Sci.* **2024**, 665, 160287.
- [27] P. G. Grützmacher, M. Cutini, E. Marquis, M. Rodríguez Ripoll, H. Riedl, P. Kutrowatz, S. Bug, C.-J. Hsu, J. Bernardi, C. Gachot, A. Erdemir, M. C. Righi, *Adv. Mater.* **2023**, 35, 2302076.
- [28] H. Zhang, N. M. Abbasi, B. Wang, in *Semiconducting Black Phosphorus: From 2D Nanomaterial to Emerging 3D Architecture*, CRC Press, Boca Raton **2021**.
- [29] J. R. Brent, N. Savjani, E. A. Lewis, S. J. Haigh, D. J. Lewis, P. O’Brien, *Chem. Commun.* **2014**, 50, 13338.
- [30] Z. Wang, P. X.-L. Feng, *2D Mater.* **2015**, 2, 021001.
- [31] H. Du, X. Lin, Z. Xu, D. Chu, *J. Mater. Chem. C* **2015**, 3, 8760.
- [32] K. L. Kuntz, R. A. Wells, J. Hu, T. Yang, B. Dong, H. Guo, A. H. Woomeer, D. L. Druffel, A. Alabanza, D. Tománek, S. C. Warren, *ACS Appl. Mater. Interfaces* **2017**, 9, 9126.
- [33] A. Ambrosi, Z. Sofer, M. Pumera, *Angew. Chem., Int. Ed.* **2017**, 56, 10443.
- [34] X. Ren, X. Yang, G. Xie, F. He, R. Wang, C. Zhang, D. Guo, J. Luo, *npj 2D Mater. Appl.* **2021**, 5, 44.

- [35] D. Flak, Q. Chen, B. S. Mun, Z. Liu, M. Rękas, A. Braun, *Appl. Surf. Sci.* **2018**, *455*, 1019.
- [36] P. C. J. Graat, M. A. J. Somers, *Appl. Surf. Sci.* **1996**, *100–101*, 36.
- [37] A. P. Grosvenor, B. A. Kobe, M. C. Biesinger, N. S. McIntyre, *Surf. Interface Anal.* **2004**, *36*, 1564.
- [38] M. Khurram, Z. Sun, Z. Zhang, Q. Yan, *Inorg. Chem. Front.* **2020**, *7*, 2867.
- [39] G. Tiouitchi, M. A. Ali, A. Benyoussef, M. Hamedoun, A. Lachgar, M. Benaïssa, A. Kara, A. Ennaoui, A. Mahmoud, F. Boschini, H. Oughaddou, A. El Kenz, O. Mounkachi, *Mater. Lett.* **2019**, *236*, 56.
- [40] C. C. Mayorga-Martinez, Z. Sofer, D. Sedmidubský, J. Luxa, B. Kherzi, M. Pumera, *Nanoscale* **2018**, *10*, 1540.
- [41] G. Zhao, T. Wang, Y. Shao, Y. Wu, B. Huang, X. Hao, *Small* **2017**, *13*, 1602243.
- [42] F. P. Bowden, D. Tabor, in *The Friction and Lubrication of Solids*, Clarendon Press **2001**, ISBN: 0-19-850777-1.
- [43] A. Favron, E. Gauffrès, F. Fossard, A.-L. Phaneuf-L'Heureux, N. Y.-W. Tang, P. L. Lévesque, A. Loiseau, R. Leonelli, S. Francoeur, R. Martel, *Nat. Mater.* **2015**, *14*, 826.
- [44] D. Barreca, S. Garon, E. Tondello, P. Zanella, *Surf. Sci. Spectra* **2000**, *7*, 81.
- [45] E. Wiberg, N. Wiberg, in *Inorganic Chemistry*, Academic Press **2001**, ISBN: 0-12-352651-5.
- [46] M. Ristić, M. Ivanda, S. Popović, S. Musić, *J. Non-Cryst. Solids* **2002**, *303*, 270.
- [47] C. Tao, B. Wang, G. C. Barber, J. D. Schall, H. Lan, *Lubr. Sci.* **2018**, *30*, 247.
- [48] Y. Wang, P. M. A. Sherwood, *Surf. Sci. Spectra* **2003**, *9*, 99.
- [49] M. R. Ripoll, R. Simič, J. Brenner, B. Podgornik, *Tribol. Lett.* **2013**, *51*, 261.
- [50] Q. Zhong, X. Pang, *J. Mater. Sci.* **2023**, *58*, 2068.
- [51] S. Kuriakose, T. Ahmed, S. Balendhran, V. Bansal, S. Sriram, M. Bhaskaran, S. Walia, *2D Mater.* **2018**, *5*, 032001.
- [52] L. Peng, N. Abbasi, Y. Xiao, Z. Xie, *Adv. Mater. Interfaces* **2020**, *7*, 2001538.
- [53] J. B. Benziger, R. J. Madix, *J. Catal.* **1980**, *65*, 36.
- [54] S. Lin, Y. Li, W. Lu, Y. S. Chui, L. Rogée, Q. Bao, S. P. Lau, *2D Mater.* **2017**, *4*, 025001.
- [55] X. Liu, J. D. Wood, K.-S. Chen, E. Cho, M. C. Hersam, *J. Phys. Chem. Lett.* **2015**, *6*, 773.